Quality Improvement Study

Medicine®

OPEN

Thin-slice brain CT with iterative model reconstruction algorithm for small lacunar lesions detection

Image quality and diagnostic accuracy evaluation

Xiaoyi Liu, PhD[a], Lei Chen, MD[a], Weiwei Qi, MD[a], Yan Jiang, MD[b], Ying Liu, MD[b], Miao Zhang, MD[a], Nan Hong, MD[a,*]

Abstract

This study was aimed to evaluate the image quality and lacunar lesion detection of thin-slice brain computed tomography (CT) images with different reconstruction algorithms, including filtered back projection (FBP), hybrid iterative reconstruction (HIR), and iterative model reconstruction (IMR) by comparison of routine slice images with FBP reconstruction. Sixty-one patients underwent noncontrast brain CT and images were reconstructed with a routine slice of 5.0 mm by FBP and thin slice of 1.0 mm by IMR, HIR, and FBP algorithms, respectively. Objective analyses included CT attenuation, noise, artifacts index of posterior cranial fossa, and contrast-to-noise ratio (CNR). Subjective analyses were performed according to overall image quality using a 5-point scale [1 (unacceptable) to 5 (excellent)]. In addition, lacunar lesion detection was compared in images with different reconstruction settings among 26 patients with lacunar lesions, with magnetic resonance imaging (MRI) as reference.

Thin-slice IMR images enabled the lowest noise, artifacts index, and the best CNR. Both IMR and HIR thin-slice images enabled better scores in subjective image quality than routine slice FBP images. Moreover, both thin-slice IMR and HIR images enabled higher sensitivity and positive predictive value (PPV) in lesion detection of 35-mm lacunar lesions compared with routine slice FBP images.

Thin-slice IMR images improve image quality, meanwhile yield better detection of small lacunar lesions in brain CT compared with routine slice FBP images.

Abbreviations: CNR = contrast-to-noise ratio, FBP = filtered back projection, HIR = hybrid iterative reconstruction, IMR = iterative model reconstruction, IR = iterative reconstruction, MRI = magnetic resonance imaging, PPV = positive predictive value, ROI = regions-of-interest, SD = standard deviation.

Keywords: brain, CT, image quality, iterative model reconstruction, thin slice

1. Introduction

Noncontrast brain computed tomography (CT) serves as the first-line imaging examination in daily clinical practice for assessing neurological disorders due to high sensitivity for bleeding, time efficiency, cost considerations, and wide availability of CT scanners. However, image quality of brain CT remains a challenge for lesion detection being affected by tissue contrast and lesion size,[1] which means it can be easier to detect lesions on brain CT images by optimizing tissue contrast. In addition, posterior cranial fossa imaging is another challenge for brain CT, which limited the diagnostic accuracy due to beam hardening and streak artifacts resulting from adjacent bone structures, volume averaging of rapid changes in anatomy in the Z-direction.[2,3] Previous studies indicated that thin-slice CT images were able to reduce relative artifacts of posterior fossa, and clarify subtle findings obscured by volume averaging on thick images.[4–6] However, image thickness reduction is also associated with increased noise thus to reduce low-contrast resolution further, which is fatal to depiction of brain structures. Therefore, thinner slice thickness must be balanced by an acceptable level of image quality as well as achieving better diagnostic accuracy. Although higher tube voltage and current can be used to substantially decrease image noise,[5] it is unacceptable in clinical practice due to the violation of as low as reasonably achievable (ALARA) principle. Thus, for a given radiation dose, it is desirable of thin-slice images with good low contrast resolution to achieve optimal image quality in brain CT.

During last decade, iterative reconstruction (IR) algorithms have been introduced to help reduce the quantum noise associated with the conventional filtered back projection (FBP) algorithms and maintain the image quality, particularly in low-dose conditions. Previous studies have demonstrated that images acquired with hybrid-type IR (HIR) algorithms, including most of the commercial available IR techniques, can maintain image quality with a certain reduction of radiation dose,[6–10] however, and have a limited ability of image noise and artifacts

Editor: Bernhard Schaller.

We declare that we have no financial and personal relationships with other people or organizations that can inappropriately influence our work, there is no professional or other personal interest of any nature or kind in any product, service, and/or company that could be construed as influencing the position presented in, or the review of, the manuscript.

The authors have no conflicts of interest to disclose.

[a] Department of Radiology, Peking University People's Hospital, Beijing, [b] Clinical Science, Philips Healthcare, Shanghai, China.

[*] Correspondence: Nan Hong, Department of Radiology, Peking University People's Hospital, Beijing 100044, China (e-mail: hongnan@bjmu.edu.cn).

Medicine (2017) 96:51(e9412)

Received: 29 July 2017 / Received in final form: 26 November 2017 / Accepted: 28 November 2017

http://dx.doi.org/10.1097/MD.0000000000009412

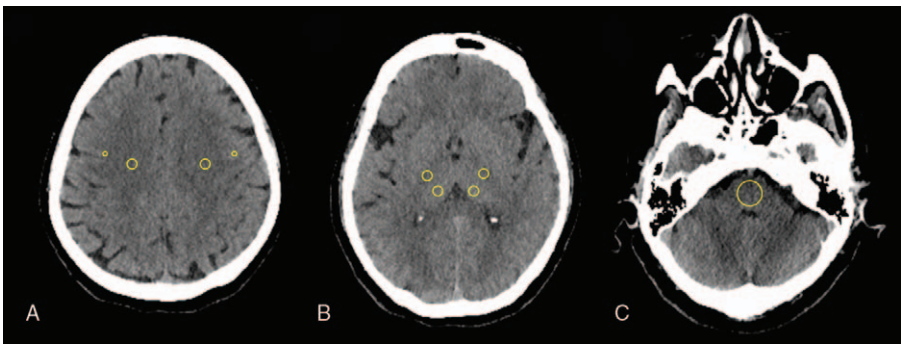

Figure 1. ROI placement. (A) Axial CT image at the level of centrum semiovale shows ROI at the following locations: deep WM and adjacent cortical GM (yellow circles). (B) Axial CT at the level of basal ganglia shows ROI at the following locations: thalamic deep GM and WM of the posterior limb of the internal capsule (yellow circles). (C) Axial CT at the posterior cranial fossa shows that ROI was placed at the obvious beam-hardening and/or streak artifacts (yellow circles).

suppression.[11] In recent years, iterative model reconstruction (IMR; Philips Healthcare, Cleveland, OH), a new advanced IR algorithm, has been introduced to enable further dose reduction and image quality improvements in brain, cardiac, chest, and abdominal studies.[7,12–18] Among which, a recent study[18] reported that IMR yielded significant better image quality in thin-slice thickness brain CT images. Thus, we assumed that IMR has the potential to balance the improvement and deterioration of image quality due to thinner slice, and designed this study to evaluate the image quality of thin-slice brain CT images reconstructed by IMR and further to investigate the lesion detection ability of thin-slice brain images with IMR, using magnetic resonance imaging (MRI) as reference.

2. Materials and methods

The study was approved by the University review board; informed consent was waived.

2.1. Patient characteristics

Sixty-one consecutive patients (33 male, 28 female; mean age, 45.2 ± 14.43 years) between June 2014 and October 2014, without obvious neuropathology findings in the CT imaging, or any complaint of headache, dizziness, and weakness, were retrospectively reviewed. In addition, 26 patients (17 male, 9 female; mean age, 60.2 ± 22.28 years) in the 61 ones, who were with presumed lacunar transient ischemic attacks or stroke, and also underwent MRI scans within 7 days, were reviewed for lacunar lesion detection, with MRI as reference. Patients with trauma, tumor, stroke, and bleeding were excluded to avoid the brain image characteristic being affected.

2.2. CT acquisitions, image reconstruction, and radiation dose

All patients were examined on a 256-slice CT system (Brilliance iCT; Philips Healthcare, Cleveland, OH). The scan parameters were as follows: detector collimation, 64 × 0.625 mm; rotation time, 0.5 seconds; pitch, 0.391; fields of view, 250 mm; tube voltage, 120 kV, tube current-time product, 300 mAs, matrix 512 × 512.

The raw data were reconstructed with FBP algorithm at 5.0 mm slice thickness and 2.5 mm interval as clinical routine. In addition, raw data were reconstructed with FBP, HIR, and IMR algorithms at 1.0 mm slice thickness and 0.5 mm interval, respectively. Thus, 4 image datasets were acquired for each patient as follows: FBP-5 mm, FBP-1 mm, HIR-1 mm, and IMR-1 mm. For HIR, we applied a moderate level (level set to 4), while for the IMR, we targeted a soft tissue setting with the mildest noise reduction (L1-Head-Routine). The FBP and HIR reconstructions were performed by host, while the IMR reconstructions were performed by a prototype. The reconstruction time for FBP was about 33 images per seconds, and 24 images per seconds for HIR. The reconstruction time of 1.0 mm slice thickness IMR images takes approximately 5 minutes per series using the prototype.

The mean volume CT dose index ($CTDI_{vol}$) was 41.4 mGy and mean dose length product (DLP) was 706.1 mGy*cm for each patient.

2.3. Image analysis

2.3.1. Objective image quality. All images were reviewed and interpreted on a dedicated CT workstation using commercially available workstation (IntelliSpace Portal version 4.0; Philips Healthcare). For evaluation of the gray matter-white matter (GM-WM) contrast, 4 bilateral regions-of-interest (ROIs) were measured: semi-oval center deep WM and adjacent cortical GM, thalamic deep GM at the level of the basal ganglia, and WM of the posterior limb of the internal capsule at the level of the basal ganglia. To assess image quality in the posterior cranial fossa, another ROI was located in the region of the posterior cranial fossa on the slice with the highest degree of beam-hardening and/or streak artifact.[19,20] Locations of these ROIs are shown in Fig. 1. We used a ROI size of 30 mm^2 for all WM locations and for deep thalamic GM, 4 to 5 mm^2 for the GM at the level of the semi-oval center, and about 200 mm^2 for the posterior cranial fossa. CT numbers of gray matter at the level of the basal ganglia was defined as average CT attenuation. Image noise was defined as the average standard deviation (SD) of the attenuation value of lateral ventricular. The posterior cranial fossa artifact index was quantified as the SD in the posterior cranial fossa ROI, which reflects the amount of fluctuation in CT numbers form beam-hardening and/or streak artifact.[19,20] Gray-white matter differentiation was measured as the contrast-to-noise ratio (CNR) between GM and WM ROIs using the following formula: $(\text{mean } HU_{GM} - \text{mean } HU_{WM})/[(\text{mean SD } HU_{GM})^2 + (\text{mean SD } HU_{WM})^2]^{1/2}$. CNR at both centrum semi-oval level and basal ganglia level were measured.

Table 1

Comparison of objective image quality among different datasets.

Datasets	Average CT attenuation of GM, HU	Image noise, HU	Artifact index, HU	CNR	
				Centrum semi-oval level	Basal ganglia level
FBP-5 mm	35.8 ± 0.17	4.33 ± 0.08	6.02 ± 0.09	1.70 ± 0.06	0.85 ± 0.03
FBP-1 mm	36.2 ± 0.23	10.10 ± 0.17	12.16 ± 0.18	1.10 ± 0.04	0.38 ± 0.02
HIR-1 mm	36.1 ± 0.23	7.02 ± 0.13	8.70 ± 0.13	1.36 ± 0.05	0.51 ± 0.02
IMR-1 mm	36.3 ± 0.17	3.69 ± 0.03	5.12 ± 0.09	2.09 ± 0.07	1.00 ± 0.30
P	.458	<.001	<.001	<.001	<.001

Data are mean ± standard deviation.

FBP = filtered back reconstruction, HIR = hybrid iterative reconstruction, IMR = iterative model reconstruction.

2.3.2. Subjective image quality. Subjective image quality assessment were performed by 2 experienced radiologists (15 and 5 years in neuroradiology) who were blinded to the reconstruction settings, according to the features of artifacts, image noise, visualization of structure, and diagnostic acceptability,[21] using a 5-point scale: 5, excellent, optimal image; 4, above average; 3, probably acceptable; 2, only acceptable under limited conditions; 1, unacceptable. When the 2 radiologists disagreed, a third neuroradiologist with >20 years of experience was asked to adjudicate the differences in order to obtain a consensus score. Images were viewed, on a brain window setting (window width, 80 HU; window level, 40 HU).

2.3.3. Lacunar lesions detection. Evaluation of lacunar lesions in CT and MRI images were performed at PACS workstation (Centricity; GE Healthcare). Two experienced radiologists (15 and 5 years in neuroradiology) were blinded to the reconstruction technique analyzed CT data and another 2 radiologists with 8 and 20-year experience in neuroradiology read MRI data. Discrepancies between 2 radiologists, in terms of lesion detection and measurement, were resolved by consensus interpretation, separately for CT and MRI images. For this study, the lacunar infarcts were detected in the basal ganglia, internal capsule, and thalamus in the level of body of the lateral ventricles, and were divided into 2 categories according to size (category I: 3 mm < maximum diameter <= 5 mm; category II: 5 mm < maximum diameter <= 15 mm). True positive lesions refer to those CT-detected lesions, meanwhile confirmed by MRI; false-positive lesions refer to those CT-detected lesions but not detected in MRI; false-negative lesions refer to those lesions confirmed by MRI but not detected in CT. Sensitivity (SEN) is defined as the proportion of true positive lesions among all positive lesions confirmed by MRI (true positive lesions and false-negative lesions); positive predictive value (PPV) is defined as the proportion of true positive lesions among all positive lesions detected by CT (true positive lesions and false-positive lesions).

2.4. Statistical analysis

All statistical analyses were performed with SPSS version 21.0 (Inc.Chicago, IL) and MedCalc (medcalc for Windows, version15.2, www.medcalc.org). All continuous values are expressed as mean ± SD. The repeated 1-way analysis of variance test was used to compare the average CT attenuation, image noise, artifact index, and CNR among different datasets, and if there was a significant difference, pairwise comparisons would be performed using the paired *t* test with the Bonferroni correction. Friedman test was used to compare subjective scores among images with different datasets, and if there was a significant difference, pairwise comparisons would be performed with the Steel–Dwass test. Interobserver agreement for subjective image scores was measured using Kappa test. McNemar test was used to compare the difference in lacunar lesion detection between the 3 groups of thin-slice images and routine slice images, respectively. A $P < .05$ was considered statistical significant.

3. Results

3.1. Objective analysis

Results of the objective assessment are summarized in Table 1 and Fig. 2. When compared with routine slice of FBP images as a reference, thin slice of IMR images enabled significant lower noise, artifact index, and improved CNRs ($P < .01$), and thin slice of FBP and HIR demonstrated significant higher noise and decreased CNRs ($P < .01$). There were no significant differences in average CT attenuation among the thin slice of FBP, HIR, and IMR images compared with routine slice of FBP images ($P = .458$).

3.2. Subjective analysis

The subjective assessment results are summarized in Table 2 and Fig. 3. There was no significant disagreement between the 2 readers (kappa value = 0.425–0.723). When compared with routine slice FBP images, both thin-slice IMR and HIR images enabled significant better scores, thin slice of FBP images demonstrated significant lower image quality scores, and failed in the diagnostic acceptable image quality.

3.3. Lacunar lesions detection

Twenty-six patients were identified with 41 lacunar lesions on MRI, including 27 lesions with a diameter of 3 to 5 mm and 14 lesions with a diameter of 5 to 15 mm. The results of lesion detection among different datasets are summarized in Table 3. Representative cases are shown in Fig. 4. For Category I lesions, both thin-slice IMR and HIR images enabled significant higher SEN and PPV than routine slice FBP images, although no difference was found in SEN and PPV between thin-slice and routine slice FBP images. For Category II lesions, no difference was found in SEN and PPV on thin-slice IMR, HIR, and FBP images when compared with routine slice FBP images, respectively.

4. Discussion

To our best knowledge, this is the first clinical study to directly compare image quality characteristics as well as lacunar lesion

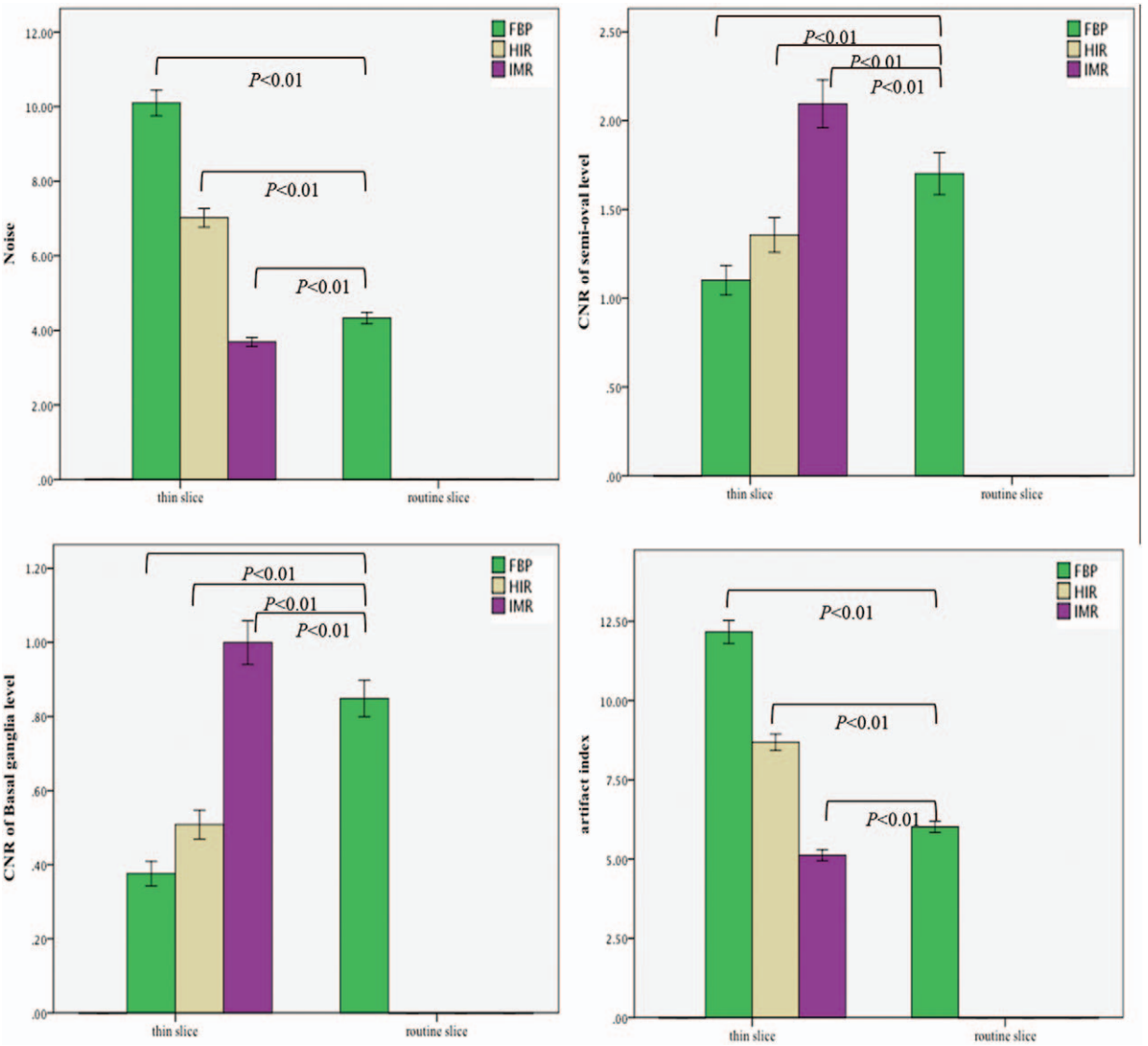

Figure 2. Data show the objective assessment among different datasets. Thin-slice IMR images enabled lowest image noise, artifacts index, and highest CNR among different datasets.

detection ability of thin-slice brain CT images with different reconstruction algorithms compared with routine images. Similar to previous studies,[17,18] our results demonstrated that thin-slice brain CT images by the use of IMR yielded better objective image quality in terms of image noise, artifacts index, and CNR as well as better subjective image quality when compared with routine images; moreover, our results also revealed that thin-slice images with IMR yielded higher SEN and PPV in detection of small lacunar lesions.

Table 2

Comparison of subjective image quality score among different datasets.

Datasets	Reader1	Reader2	Kappa	Final
FBP-5 mm	0/17/42/2/0	0/16/42/3/0	0.723	0/18/41/2/0
FBP-1 mm	0/5/46/10/0	0/2/45/14/0	0.425	0/3/48/10/0
HIR-1 mm	1/24/36/0/0	1/30/30/0/0	0.631	0/30/31/0/0
IMR-1 mm	22/33/6/0/0	17/40/4/0/0	0.694	17/41/3/0/0

Data show the frequency of numerical scores given in each category (grade 5/4/3/2/1).
FBP = filtered back projection, HIR = hybrid iterative reconstruction, IMR = iterative model reconstruction.

In theory, slice thickness has a strong linear influence on the number of photons used to produce the images, and thinner slices use less photons resulting in increased image noise and deteriorated low-contrast resolution,[22] which is fatal to differentiating the grey and white matters in brain CT images. In routine brain CT images, the difference of CT number between the gray and white matter is very small (typically from 5 to 10 HU difference); hence, image noise can affect image quality significantly and should be limited less than 5 HU.[23] Usually, thin-slice images with significant increased noise cannot be used for clinical diagnosis; however, we found that by use of IMR, image noise that low enough was achieved in thin-slice images, while thin-slice images reconstructed with HIR and FBP both failed in limiting image noise less than 5 HU. In addition, beam

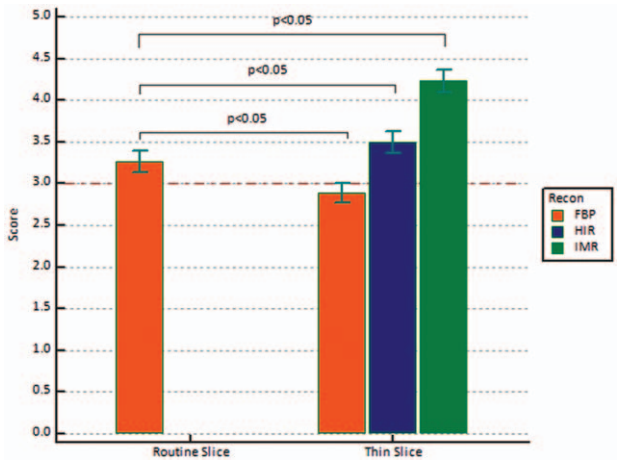

Figure 3. Comparison of subjective image quality score among different datasets. Both thin-slice IMR and HIR images enabled better image quality than routine slice FBP images. Thin-slice FBP images failed in the diagnostic acceptable image quality.

Table 3

Comparison of lacunar lesion detection among different datasets.

Lesion category	Datasets	TP (n)	FP (n)	FN (n)	SEN (%)	PPV (%)	*P*
I (3–5 mm)	FBP-5 mm	7	4	20	25.9	63.6	n/a
	FBP-1 mm	14	10	13	51.8	58.3	.065
	HIR-1 mm	16	7	11	59.3	69.5	.012
	IMR-1 mm	18	4	9	66.7	81.8	.003
II (5–15 mm)	FBP-5 mm	10	0	4	71.4	100	n/a
	FBP-1 mm	10	0	4	71.4	100	1.000
	HIR-1 mm	10	0	4	71.4	100	1.000
	IMR-1 mm	12	0	2	85.7	100	.625

Data are number of cases and the percentage.

FN = false negative, FP = false positive, PPV = positive predictive value, SEN = sensitivity, TP = true positive.

hardening and streak artifacts in posterior cranial fossa region were found significantly reduced on thin-slice IMR images. Beam hardening and streak artifacts in posterior cranial fossa are mainly caused by adjacent bone structures in the region and partial volume effect of thick slice reformatting of images. Previous studies have used various reconstruction algorithms to decrease noise and these artifacts in this region.[24,25] Machida et al[25] indicated the utility of model-based IR improved delineation of arteries in the posterior fossa than FBP technique. Thus, in our study, the artifacts reduction in posterior fossa region can be attributed to thinner slice helps for posterior fossa related artifacts reduction and the superior capability of IMR in noise reduction.

For subjective image quality, we found that both IMR and HIR thin-slice images enabled better score than routine images despite HIR demonstrated a higher image noise and artifact index as well as lower CNR than routine images, which implies that thinner slice images enabled the advantages in subtle findings depiction and posterior fossa related artifacts reduction to balance the deteriorated image quality due to decreased low-contrast resolution.

Similar to subjective image quality, we found both IMR and HIR thin-slice images enabled better diagnostic performance including SEN and PPV than routine images in detection of small lacunar lesions (diameter less than 5 mm); however, no difference was found in detection of larger lacunar lesion (diameter more than 5 mm). Obviously, small lesions might be missed on routine images with a slice thickness of 5 mm due to partial volume effect, which is the main reason for thin-slice images to demonstrate better detection ability in small lesions. In addition, improved

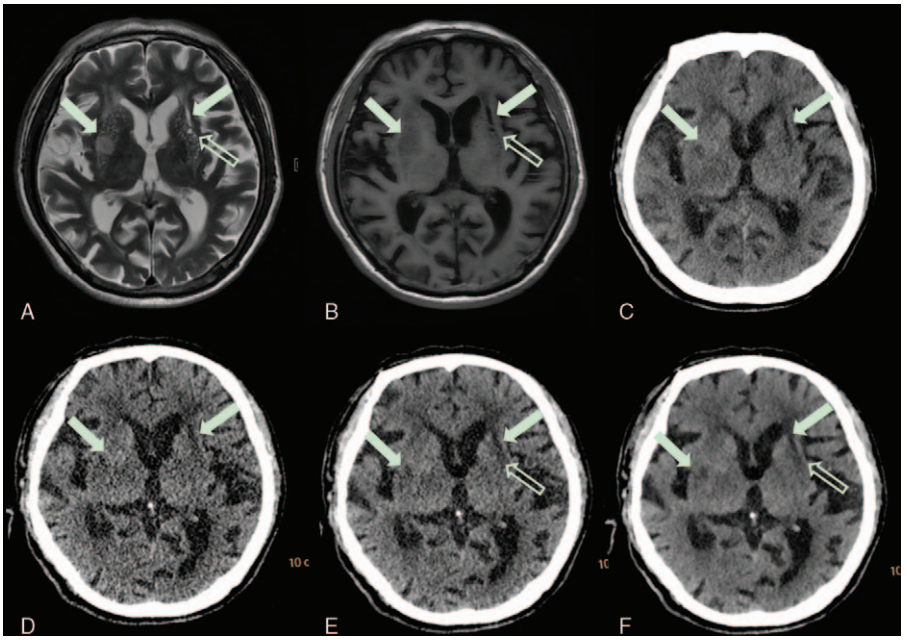

Figure 4. Brain MR and CT images in a 79-year-old man. T2WI (A), T1WI (B), routine slice FBP (C), thin slice FBP (D), thin-slice HIR (E), and thin-slice IMR (F). Large lesion with size 6–15 mm in bilateral basal ganglia (solid arrow) and 1 small lesion with size 3–5 mm in left basal ganglia were confirmed on MR image (open arrow). The large lesions were well visualized on routine slice FBP image and all thin-slice images with 3 reconstruction algorithms. The 2 small lacunar lesions were well depicted on thin-slice IMR than and HIR images; however, it was not identified on corresponding routine and thin-slice FBP image. According to the small lesion detection and overall image quality, thin-slice IMR image could be the most appropriate reconstruction algorithm.

CNR and better depiction of small lesion were possible reasons for higher diagnostic performance of IMR in small lesion detection. Moreover, it is worth noting that HIR thin-slice images in addition to IMR thin-slice images enabled significant better diagnostic performance in small lesion detection indicated that slice thickness optimization in addition to noise reduction might be the key features to improve diagnostic performance of brain CT. However, CT is not ideal or noise free, small lacunar lesion is prone to be false positive or missed detection, routine images enabled a SEN of only 25.9%, and a PPV of 63.6%; even on IMR thin-slice images, the SEN and PPV was only 66.7% and 81.8%, respectively. As for larger lesions, significant better diagnostic accuracy in lesion detection was achieved in all 4 CT datasets; thus, the advantages were not easy to demonstrate for certain image series.

We also investigated the reconstruction time of thin-slice images reconstructed with different algorithms. As we all know, it costs more time for thin-slice image reconstruction due to larger amount of data processing. Meanwhile, IMR is a new kind of full IR algorithm without blending of FBP. It uses a knowledge-based approach to accurately determine the data, image statistics, and the system models of CT scanner, and produces optimal images by iteratively minimizing the difference between acquired data and their ideal form.[26] Theoretically, image noise can be removed from the modelled projection data in a final IMR step, resulting in an artifact- and noise-free image, and the iterative procedures produced large amount of data processing. Accordingly, thin-slice IMR images need longer reconstruction time. Previous study[27] indicated that early model-based IR algorithms with similar large amount of data processing cost too much time to practice in clinical, while in our study, we observed that the reconstruction time of IMR is clinical acceptable, taking approximately 5 minutes for each thin-slice series. In our hospital, thin-slice IMR of brain CT is used routinely on a clinical basis.

Our study has several limitations. First, we did not investigate thin-slice images at a low-dose condition, the superior capability of IMR in noise reduction may provide acceptable image quality and diagnostic performance at low dose scans, and further studies need to be implemented; Second, a relative small number of patients were included in our study, which may result in some deviations, but it should not influence the study results. Third, due to the difference of imaging principle, CT may have lower sensitivity than MRI in detection of lacunar lesion; however, it is worth to investigate the approaches improving CT diagnostic accuracy and CT has been significantly improved in small lesion detection than last decades. Fourth, the study only included patients with lacunar transient ischemic attacks or stroke. Further studies are required to evaluate the effects of IMR on brain tumors detection, grading, and differential diagnosis.[28]

5. Conclusion

Thin-slice brain CT images by use of IMR improve image quality and enable better sensitivity as well as PPV in detection of small lacunar lesion, which implies IMR may have the potential to demonstrate more subtle abnormalities of brain and hiding lesions.

References

[1] von Kummer R, Bourquain H, Bastianello S, et al. Early prediction of irreversible brain damage after ischemic stroke at CT. Radiology 2001;219:95–100.

[2] Heuscher DJ, Vembar M. Reduced partial volume artifacts using spiral computed tomography and an integrating interpolator. Med Phys 1999;26:276–86.

[3] Jones TR, Kaplan RT, Lane B, et al. Single- versus multi-detector row CT of the brain: quality assessment. Radiology 2001;219:750–5.

[4] Singh S, Kalra MK, Hsieh J, et al. Abdominal CT: comparison of adaptive statistical iterative and filtered back projection reconstruction techniques. Radiology 2010;257:373–83.

[5] Tang K, Wang L, Li R, et al. Effect of low tube voltage on image quality, radiation dose, and low-contrast detectability at abdominal multidetector CT: phantom study. J Biomed Biotechnol 2012;2012: 130169.

[6] Lin XZ, Machida H, Tanaka I, et al. CT of the pancreas: comparison of image quality and pancreatic duct depiction among model-based iterative, adaptive statistical iterative, and filtered back projection reconstruction techniques. Abdom Imaging 2014;39:497–505.

[7] Khawaja RDA, Singh S, Otrakji A, et al. Dose reduction in pediatric abdominal CT: use of iterative reconstruction techniques across different CT platforms. Pediatr Radiol 2015;45:1046–55.

[8] Bodelle B, Wichmann JL, Scholtz JE, et al. Iterative reconstruction leads to increased subjective and objective image quality in cranial CT in patients with stroke. AJR Am J Roentgenol 2015;205:618–22.

[9] Nishizawa M, Tanaka H, Watanabe Y, et al. Model-based iterative reconstruction for detection of subtle hypoattenuation in early cerebral infarction: a phantom study. Jpn J Radiol 2015;33:26–32.

[10] Katsura M, Sato J, Akahane M, et al. Comparison of pure and hybrid iterative reconstruction techniques with conventional filtered back projection: image quality assessment in the cervicothoracic region. Eur J Radiol 2013;82:356–60.

[11] Oda S, Utsunomiya D, Funama Y, et al. A hybrid iterative reconstruction algorithm that improves the image quality of low-tube-voltage coronary CT angiography. Am J Roentgenol 2012;198:1126–31.

[12] Li T, Zhang Y, Wang Y, et al. Chest CT with iterative reconstruction algorithms for airway stent evaluation in patients with malignant obstructive tracheobronchial diseases. Medicine (Baltimore) 2016;95: e4873.

[13] Oda S, Weissman G, Vembar M, et al. Iterative model reconstruction: improved image quality of low-tube-voltage prospective ECG-gated coronary CT angiography images at 256-slice CT. Eur J Radiol 2014;83:1408–15.

[14] Suzuki S, Haruyama T, Morita H, et al. Initial performance evaluation of iterative model reconstruction in abdominal computed tomography. J Comput Assist Tomogr 2014;38:408–14.

[15] Yoon JH, Lee JM, Yu MH, et al. Comparison of iterative model-based reconstruction versus conventional filtered back projection and hybrid iterative reconstruction techniques: lesion conspicuity and influence of body size in anthropomorphic liver phantoms. J Comput Assist Tomogr 2014;38:859–68.

[16] Oda S, Weissman G, Vembar M, et al. Cardiac CT for planning redo cardiac surgery: effect of knowledge-based iterative model reconstruction on image quality. Eur Radiol 2015;25:58–64.

[17] Love A, Olsson ML, Siemund R, et al. Six iterative reconstruction algorithms in brain CT: a phantom study on image quality at different radiation dose levels. Br J Radiol 2013;86:20130388.

[18] Nakaura T, Iyama Y, Kidoh M, et al. Comparison of iterative model, hybrid iterative, and filtered back projection reconstruction techniques in low-dose brain CT: impact of thin-slice imaging. Neuroradiology 2016;58:245–51.

[19] Pomerantz SR, Kamalian S, Zhang D, et al. Virtual monochromatic reconstruction of dual-energy unenhanced head CT at 65-75 keV maximizes image quality compared with conventional polychromatic CT. Radiology 2013;266:318–25.

[20] Riordan AJ, Bennink E, Viergever MA, et al. CT brain perfusion protocol to eliminate the need for selecting a venous output function. AJNR Am J Neuroradiol 2013;34:1353–8.

[21] EUR 16252. Tomography European Guidelines Quality Criteria 2004. Available at: www.drs.dk/guidelines/ct/quality/.

[22] Bushberg JT, Seibert JA, Leidholdt EM, et al. The Essential Physics of Medical Imaging. 2nd ed.2002;Lippincott Williams & Wilkins, Philadelphia, PA:369.

[23] Awai K, Higaki T, Tatsugami F. Clinically essential requirement for brain CT with iterative reconstruction. Br J Radiol 2014;87: 20140474.

[24] Kilic K, Erbas G, Guryildirim M, et al. Lowering the dose in head CT using adaptive statistical iterative reconstruction. Am J Neuroradiol 2011;32:1578–82.

[25] Machida H, Takeuchi H, Tanaka I, et al. Improved delineation of arteries in the posterior fossa of the brain by model-based iterative reconstruction in volume-rendered 3D CT angiography. AJNR Am J Neuroradiol 2013;34:971–5.
[26] Mehta D, Thompson R, Morton T, et al. Iterative model reconstruction: simultaneously lowered computed tomography radiation dose and improved image quality. Med Phys Int J 2013;2:147–54.
[27] Miéville FA, Gudinchet F, Brunelle F, et al. Iterative reconstruction methods in two different MDCT scanners: physical metrics and 4-alternative forced-choice detectability experiments: a phantom approach. Phys Med 2013;29:99–110.
[28] Schaller BJ, Cornelius JF, Sandu N, et al. Molecular imaging of brain tumors personal experience and review of the literature. Curr Mol Med 2008;8:711–26.